

Crystal Morphology and Optical Emissions of GaN layers grown on Si(111) substrates by Molecular Beam Epitaxy

M. A. Sánchez-García¹, F. J. Sánchez¹, F. B. Naranjo¹, F. Calle¹, E. Calleja¹, E. Muñoz¹, U. Jahn² and K. H. Ploog²

¹Dpt. Ingeniería Electrónica, E.T.S.I. Telecomunicación, Politécnica, Ciudad Universitaria,

²Paul-Drude-Institut für Festkörperelektronik,

(Received Monday, June 22, 1998; accepted Wednesday, October 7, 1998)

Crystal morphology of GaN layers grown on Si(111) evolves from whisker-like microcrystals to compact films as a function of the III/V ratio. Small changes in the III/V ratio (from Ga-rich to N-rich) during the growth of a compact layer result in the appearance of microcrystals on the top of the layer, indicating a sharp transition between the two growth regimes.

Four different morphologies are obtained by increasing the III/V ratio: a) completely columnar whisker-like samples exhibiting a pair of intense excitonic emissions at 3.471-3.478 eV; b) a mixture of compact regions with columnar microcrystals showing two pairs of excitonic emissions; c) compact layers with very small microcrystals on the top surface with a weaker dominant transition at 3.415 eV (± 5 meV) and, d) full compact and smooth layers with a single dominant excitonic emission at 3.466 eV. A combination of PL measurements with SEM photographs and CL imaging reveals that both pairs of emissions in samples b) come from the columnar microcrystals. The high energy pair (3.471-3.478eV) is attributed to the free-exciton A and a donor-bound exciton while the low energy pair (3.452-3.458eV) is assigned to acceptor-bound excitons associated to valence bands Γ_{9v} and Γ_{7uv} . Power and temperature dependence together with time-resolved data show that the dominant peak at 3.415eV (± 5 meV) present in samples c) correspond to a donor-acceptor transition. CL measurements as a function of electron beam energy (depth) also indicate that this emission is more intense towards the interface between the layer and the sample. Finally, the excitonic emission in samples d) is shifted to lower energies due to residual biaxial tensile strain of thermal origin.

1 Introduction

GaN has proven to be an excellent semiconductor material for application in UV/blue optoelectronic devices [1]. Although direct epitaxial growth of GaN films on Si substrates is a difficult task (mainly due to the 17% lattice mismatch present), substantial progress in the crystal quality has been achieved using AlN or GaN buffer layers [2] [3] [4]. A full characterization of the quality of the material needs to be assessed by a combination of different techniques.

In this work we report on the crystal morphology and low temperature photoluminescence (PL) of GaN layers grown by molecular beam epitaxy (MBE) on Si(111) substrates. Both the morphology and the optical properties of the films are very dependent on the III/V ratio used during growth. Scanning electron micros-

copy (SEM) and cathodoluminescence (CL) techniques are performed to establish a correlation between the growth parameters and the morphology and optical emissions present in the films. PL measurements as a function of the temperature and excitation power are also performed to identify more precisely these optical emissions.

2 Experimental Details

Wurtzite GaN films were grown on Si(111) substrates, with optimized AlN buffer layers [5], by plasma-assisted molecular beam epitaxy (MBE) using a radio frequency (RF) plasma source to activate the nitrogen. Typical growth temperatures were 850°C for the AlN buffer layer and 750°C for the GaN epilayer. The thicknesses of the samples varied between 0.8 and 1.2 μm .

Details of the growth system and substrate cleaning procedure are given elsewhere [6].

Figure 1 shows the GaN growth rate as a function of the Ga-flux (ie. the III/V ratio) for a fixed growth temperature and amount of active nitrogen. The growth rate scales with the Ga-flux (N-rich regime) until it reaches a saturation value at $0.52 \mu\text{m/h}$, beyond which Ga condensation takes place (Ga-rich regime). We will consider the stoichiometry zone (or III/V ratio close to one) that where the curve starts to saturate (encircled in Figure 1). Growth with III/V ratios below this zone will be considered N-rich samples whereas above it will be considered Ga-rich ones.

The low temperature PL was performed using the 334nm line of an Ar⁺ laser, a Jobin-Yvon THR1000 monochromator and a GaAs photomultiplier. Cathodoluminescence (CL) experiments (electron beam energy from 4 to 25 keV) were carried out in a scanning electron microscope equipped with an Oxford Mono-CL and He cooling stage system (5-300 K). A grating monochromator and a cooled photomultiplier were used in conjunction with a conventional photon counting technique to disperse and detect the CL, respectively.

3 Results and discussion

3.1 Crystal Morphology

Figure 2 shows scanning electron microscopy (SEM) photographs of GaN layers grown at 750°C with different III/V ratios. Crystal morphology of N-rich samples (sample A) is strongly columnar, formed by an array of whisker-like microcrystals of approximately 60nm diameter and $1\mu\text{m}$ long (sample A in Figure 2), similar to GaN films grown at low temperature (550°C) directly on GaAs by organometallic vapor phase epitaxy [7]. The growth of sample B in Figure 2 started with a III/V ratio close to stoichiometry (compact layer) and it was reduced during the last stage of the growth by lowering the temperature of the gallium cell (ie reducing the gallium flux). The result was a change in the morphology of the layer with the appearance of columnar microcrystals. This effect is also obtained by increasing the substrate temperature above 750°C during the growth, since gallium evaporates from the surface leading to an effective smaller III/V ratio. The surface morphology of this sample is very rough with columnar microcrystals coming out of hexagonal craters. This can be clearly seen in Figure 4. Sample C in Figure 2 was grown slightly under N-rich conditions. These growth conditions lead to the formation of small microcrystals, in rather low concentrations, on the surface of the layer. However, the roughness is highly improved compared with sample B. Sample D in Figure 2 was grown under optimal condi-

tions (slightly above stoichiometry) leading to a compact layer with a smooth surface and no microcrystals.

3.2 Optical Emissions

The optical properties of the GaN layers will be presented according to the morphology of the film. In the section devoted to morphology we defined four types of samples namely A, B, C and D (Figure 2). The dominant emissions of each type of sample will be now analyzed.

3.2.1 Sample A

Sample A corresponds to GaN layers grown under N-rich conditions. The low temperature PL spectra of these samples (Figure 3a) are dominated by a pair of intense excitonic emissions at 3.471-3.478 eV. The peak at 3.478 eV corresponds to the free exciton A, which is also observed in relaxed, thick GaN [8] and homoepitaxial GaN [9]. The 3.471 eV line is attributed to a donor-bound exciton (DBE), since it follows the expected temperature and power dependence and a binding energy of 35 meV is derived [10], in perfect agreement with the established value given by Meyer et al [11]. The strong intensity and narrow character of these emissions (<2 meV FWHM) are indicative of the high quality of these columnar microcrystals.

3.2.2 Sample B

The growth of sample B started with a III/V ratio close to stoichiometry producing a compact initial layer. Towards the end of the growth, the III/V ratio was reduced and the resulting morphology can be seen in Figure 2. The PL spectrum of this sample is dominated by two pairs of excitonic emissions (Figure 3b) at 3.450-3.456 eV and 3.471-3.478 eV. The surface morphology of sample B is quite rough and inhomogeneous. Figure 4 shows SEM photographs of three different surface zones, from the edge of the wafer towards the center. The density of columnar microcrystals decreases when moving towards the center probably due to different local substrate temperatures during growth which resulted in different III/V ratios (always in the N-rich side). Low temperature PL spectra of those three zones (Figure 5) show the same type of emissions but with decreasing intensity as the density of columns also decreases (ie. moving from the edge towards the center). This first piece of evidence could indicate that both pairs of emissions originate from the columns. Cathodoluminescence (CL) imaging for the two energy regions (3.45 and 3.47 eV) confirms unambiguously this hypothesis (Figures 6 a and b). From these images, the luminescence is shown to originate at the same spots in both cases.

The high energy pair (3.471 and 3.478 eV) is the same pair of emissions observed in sample A : donor-

bound exciton and free-exciton A characteristic of relaxed material.

From the temperature and power dependence of the emissions at 3.450 and 3.456 eV [10] and the energy separation between them, we identify these transitions with acceptor bound excitons (ABE) linked to the Γ_{9v} and Γ_{7uv} valence bands (A and B). The study of the intensity of these two emissions with temperature have lead to an activation energy of 22 meV for the exciton binding energy.

3.2.3 Sample C

The morphology of this sample presents small microcrystals on the surface of the layer (Figure 2). In general, the morphology is more compact than in sample B. The low temperature PL spectrum corresponding to this sample is shown in Figure 3c. The spectrum is dominated by an emission around 3.415 eV with smaller intensity as those of samples A and B. Similar emissions might appear at 3.405 or 3.421 eV, partially resolved, depending on the sample. We have focused our study on the emission at 3.415 eV, although the temperature and power dependence of all three emissions are similar.

The intensity of the emission at 3.415 eV is also dependent on the density of microcrystals present on the surface. Figure 7 shows top views SEM photographs of three different type-C samples exhibiting different microcrystals densities on the surface. The low temperature PL spectrum of each one of these samples is shown in Figure 8. It seems that this emission is also correlated with the density of these microcrystals. Cathodoluminescence (CL) with different electron beam energies (ie. different excitation depths) was also performed on these samples. The intensity of the broad CL line centered at 3.415 eV increases with increasing excitation depth (Figure 9). For beam energies larger than 15 keV, the whole intensity decreases, in good agreement with the thickness of the layer (Figure 10). From this measurement, it seems that the origin of this emission is more concentrated near the interface of the layer.

The emission at 3.415 eV blue-shifts with increasing excitation, its temperature dependence is very much like that expected from a DAP [11], it has a slow and strong non-exponential decay in time-resolved PL experiments ($\tau \sim 3000$ ps) and it shows fine structure [10], already reported in GaN grown on (111)B GaAs [12]. A DAP character is therefore attributed to this emission. Considering the donor related to the DBE at 3.472 eV, a band gap energy of 3.503 eV [13], and a Coulombic energy term of 15 meV, an acceptor optical energy around 70 meV is derived. Since this emission becomes stronger in N-rich samples and the acceptor binding energy derived from it is much smaller than those corre-

sponding to known acceptors [14], we can speculate about complex defects involving V_{Ga} and/or contaminants as the origin of these emissions. The Ga vacancy generally identified in MOCVD layers grown on sapphire substrates has been seen to correlate with the yellow luminescence intensity [15]. The samples of this work show no traces of the yellow band, neither at low nor at room temperature. Positron annihilation spectroscopy data from these samples detected vacancy clusters as a result of an interdiffusion process across the interface but they were not associated with simple Ga vacancies [16]. The fact that this emission (3.412 eV) is sometimes observed at slightly different energies (3.405 or 3.421 eV) could be explained based on the hypothesis of the formation of different vacancy clusters and/or complex defects involving V_{Ga} .

3.2.4 Sample D

The PL spectrum of sample D (Figure 3d) is dominated by a single excitonic emission at 3.446 eV. This emission is shifted to lower energies due to residual biaxial tensile strain of thermal origin present in the layer. The intensity of the emission has decreased by a factor of 25 compared with sample A. This reduction is easily explained by comparing the two different crystal morphologies (Figure 2). The whiskers in sample A are nearly perfect isolated crystals free of dislocations or any other non-radiative center, whereas sample D do have a large number of dislocations (of the order of 10^{10} cm^{-2}) most likely responsible of this reduction in the photoluminescence emission. The shift in the position of the peak towards lower energies, due to residual strain, is in good agreement with previous results by Chichibu et al [17].

4 Summary

In summary, the morphology and the optical properties of the GaN layers grown on Si(111) substrates are very dependent of the growth parameters, and in particular of the III/V ratio. The need of a compact layer is crucial to obtain good electrical transport properties. The quality of the material needs to be assessed by comparing different characterization techniques. It is proven that the quality of the GaN film improves highly with the use of optimized AlN buffer layers, but, the morphology of the GaN layer is mostly governed by the specific growth parameters. Small variations in the III/V ratio during the growth (either by lowering the Ga cell temperature or by increasing the substrate temperature) lead to N-rich conditions producing columnar microcrystals and different optical properties. This transition occurs very quickly once the growth conditions are outside of the stoichiometry zone.

ACKNOWLEDGMENTS

Partial funding by CYCIT MAT96-1947CE and EU ESPRIT LTR 20968 (LAQUANI) is acknowledged.

REFERENCES

- [1] S. Nakamura, M. Senoh, S. Nagahama, N. Iwasa, T. Yamada, T. Matsushita, Y. Sugimoto, H. Kiyoku, *Appl. Phys. Lett.* **69**, 4056-4058 (1996).
- [2] K. S. Stevens, A. Ohtani, A. F. Schwartzman, R. Beresford, *J. Vac. Sci. Technol. B* **12**, 1186-1189 (1994).
- [3] J. W. Yang, C. J. Sun, Q. Chen, M. Z. Anwar, M. A. Khan, S. A. Nikishin, G. A. Seryogin, A. V. Osinsky, L. Chernyak, H. Temkin, C. hu, S. Mahajan, *Appl. Phys. Lett.* **69**, 3566 (1996).
- [4] S. Guha, N. Bojarczuk, *Appl. Phys. Lett.* **72**, 26 (1998).
- [5] M. A. Sanchez-Garcia, E. Calleja, E. Monroy, F. J. Sánchez, F. Calle, E. Muñoz, A. Sanz. Hervas, C. Villar, M. Aguilar, *MRS Internet J. Nitride Semicond. Res.* **2**, 33 (1997).
- [6] M.A. Sanchez-Garcia, E. Calleja, E. Monroy, F.J. Sanchez, F. Calle, E. Muñoz, R. Beresford, *J. Cryst. Growth* **183**, 23-30 (1998).
- [7] D. K. Gaskill, N. Bottka, M. C. Lin, *Appl. Phys. Lett.* **48**, 1449-1451 (1986).
- [8] D Volm, K Oettinger, T Streibl, D Kovalev, M Ben-Chorin, J Diener, BK Meyer, J Majewski, L Eckey, A Hoffman, H Amano, I Akasaki, K Hiramatsu, T Detchprohm, *Phys. Rev. B* **53**, 16543-16550 (1996).
- [9] K Pakula, A Wyszomolek, KP Korona, JM Baranowski, R Stepniewski, I Grzegory, M Bockowski, J Jun, S Krukowski, M Wroblewski, S Porowski, *Sol. St. Comm.* **97**, 919-922 (1996).
- [10] F Calle, F J Sanchez, J M G Tijero, M A Sanchez-Garcia, E Calleja, R Berenford, *Semicond. Sci. Technol.* **12**, 1396-1403 (1997).
- [11] B. K. Meyer, D. Volm, A. Graber, H. C. Alt, T. Detchprohm, A. Amano, I. Akasaki, *Sol. St. Comm.* **95**, 597 (1995).
- [12] M. Ilegems, R. Dingle, R. A. Logan, *J. Appl. Phys.* **43**, 3797 (1972).
- [13] B. G. Ren, J. W. Orton, T. S. Cheng, D. J. Dewsnip, D. E. Lacklison, C. T. Foxon, C. H. Malloy, X. Chen, *MRS Internet J. Nitride Semicond. Res.* **1**, 22 (1996).
- [14] J W Orton, *Semicond. Sci. Technol.* **10**, 101 (1995).
- [15] K. Saarinen, T. Laine, S. Kuisma, J. Nissila, L. Dobrzynski, J. M. Baranowski, K. Pakula, R. Setpniewski, M. Wojdak, A. Wyszomolek, T. Suski, M. Leszczynski, I. Grzegory, S. Porowski, *Phys. Rev. Lett.* **79**, 3033 (1997).
- [16] E. Calleja, M. A. Sánchez-García, D. Basak, F. J. Sánchez, F. Calle, P. Youinou, E. Muñoz, J. J. Serrano, J. M. Blanco, C. Villar, T. Laine, J. Oila, K. Saarinen, P. Hautojarvi, C. H. Molly, D. J. Somerford, I. Harrison, *Phys. Rev. B* **58**, 1550 (1998).
- [17] S. Chichibu, T. Azuhata, T. Sota, H. Amano, I. Akasaki, *Appl. Phys. Lett.* **70**, 2085 (1997).

FIGURES

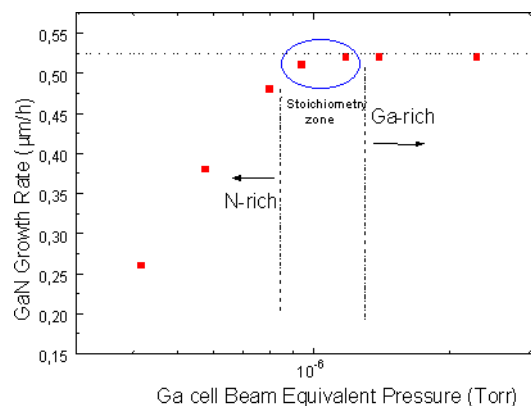


Figure 1. GaN growth rate as a function of the Ga flux (Beam Equivalent Pressure) for a fixed substrate temperature (750°C) and amount of active nitrogen. Definition of the stoichiometry zone (ie. III/V ratio ~1).

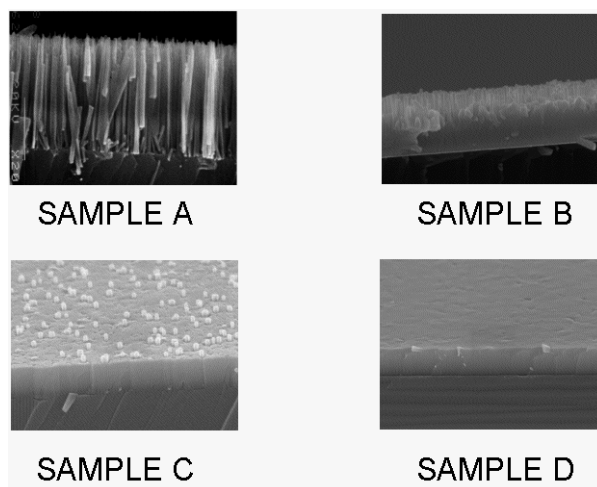


Figure 2. Cross sectional SEM photographs of GaN layers grown with different III/V ratios, from N-rich conditions (sample A) to close to stoichiometry (sample D).

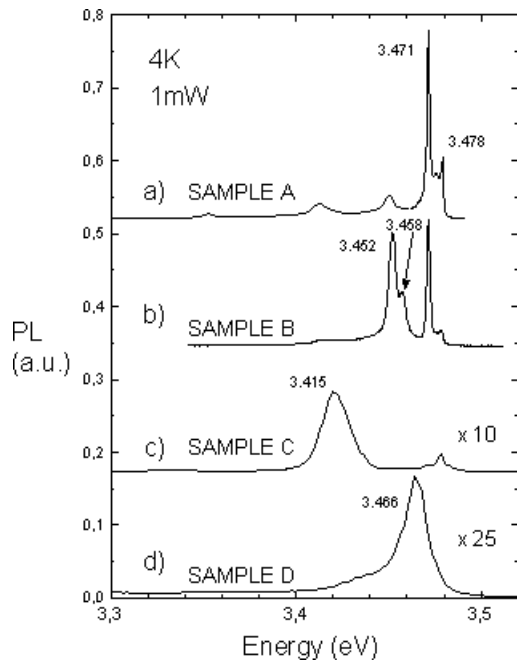


Figure 3. Low temperature PL spectra of the samples described in Figure 2.

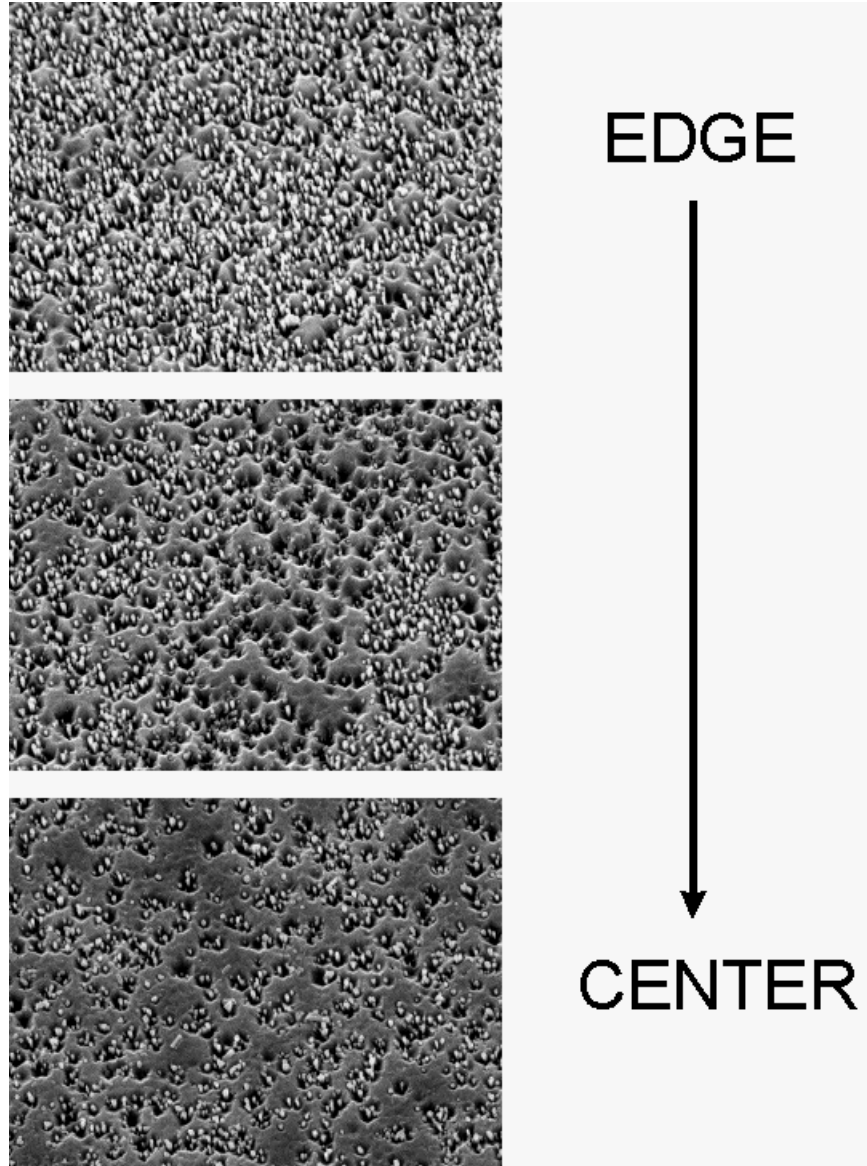


Figure 4. Top view SEM photographs of three different zones on a type-B sample, from the edge of the wafer towards the center. Notice the decrease in the density of columnar microcrystals.

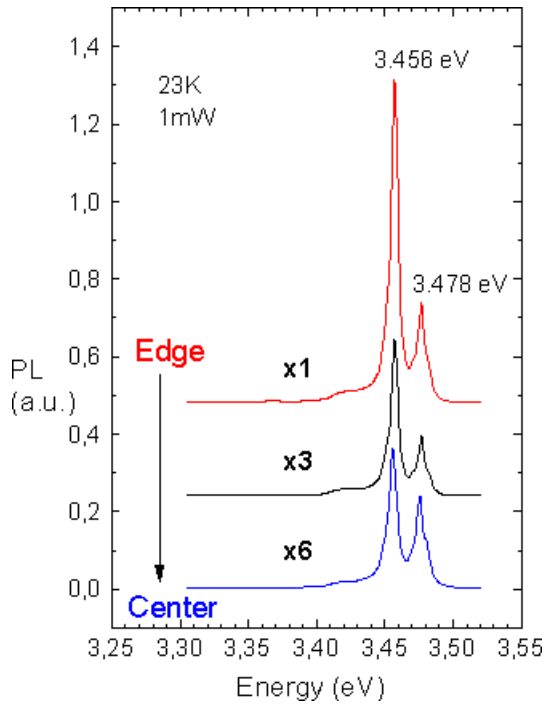


Figure 5. Low temperature PL of the three zones described in Figure 4, from the edge to the center of the wafer.

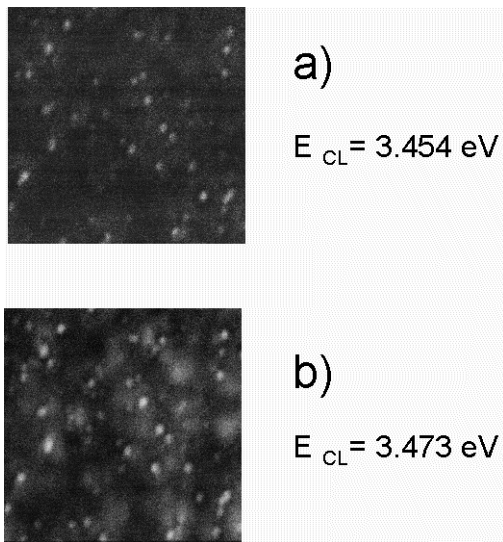


Figure 6. Cathodoluminescence imaging of a type-B sample for two energies : a) 3.454 and b) 3.473 eV.

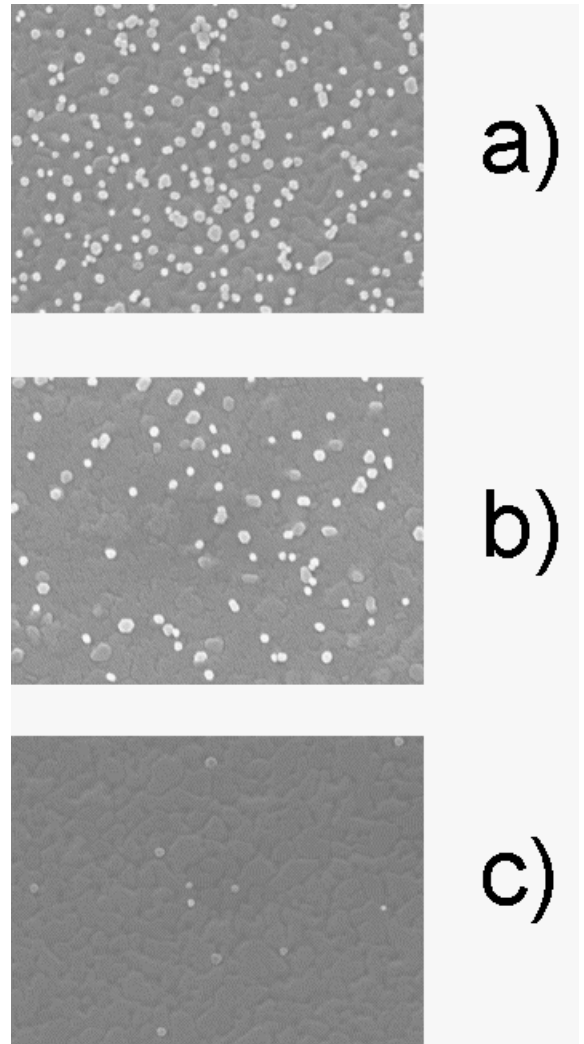


Figure 7. Top views SEM photographs of three different type-C samples exhibiting different microcrystals densities on the surface.

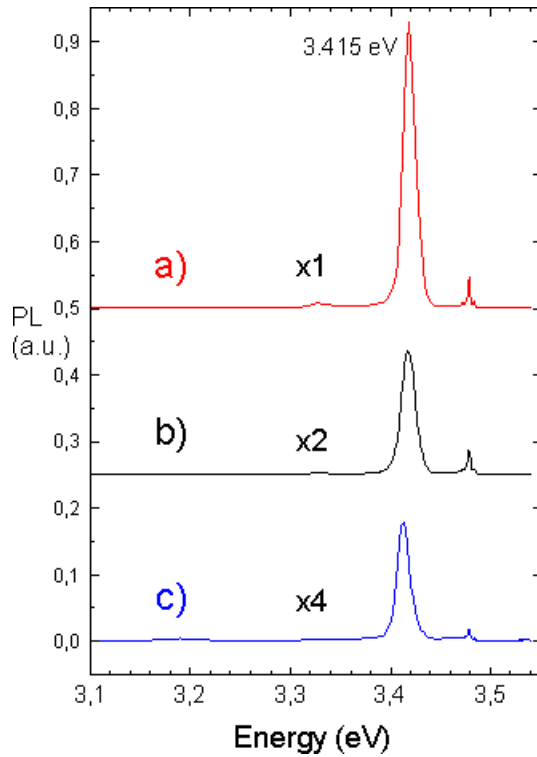


Figure 8. Low temperature PL of the three samples described in Figure 7.

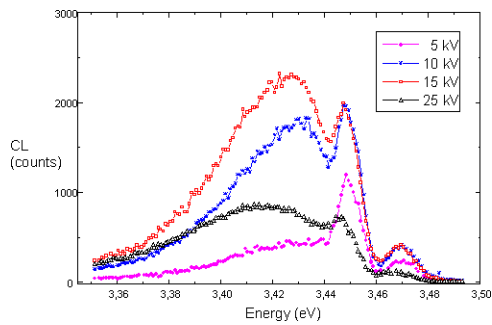


Figure 9. Cathodoluminescence of a type-C sample with electron beam energies from 5 to 25 keV (ie different excitation depths).

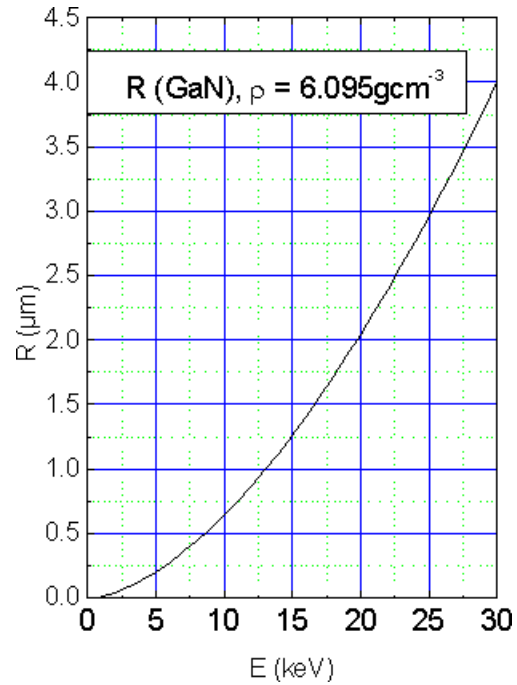


Figure 10. Calculated excitation depth as a function of electron beam energy for GaN